

Application of an optimization algorithm to satellite ocean color imagery: A case study in Southwest Florida coastal waters

Chuanmin Hu^{1*}, Zhongping Lee², Frank E. Muller-Karger¹, Kendall L. Carder¹

¹College of Marine Science, Univ. of South Florida, 140 7th Ave. S., St. Petersburg, FL 33701, USA

²Naval Research Laboratory, Stennis Space Center, MS 39529, USA

ABSTRACT

A spectra-matching optimization algorithm, designed for hyperspectral sensors, has been implemented to process SeaWiFS-derived multi-spectral water-leaving radiance data. The algorithm has been tested over Southwest Florida coastal waters. The total spectral absorption and backscattering coefficients can be well partitioned with the inversion algorithm, resulting in RMS errors generally less than 5% in the modeled spectra. For extremely turbid waters that come from either river runoff or sediment resuspension, the RMS error is in the range of 5-15%. The bio-optical parameters derived in this optically complex environment agree well with those obtained *in situ*. Further, the ability to separate backscattering (a proxy for turbidity) from the satellite signal makes it possible to trace water movement patterns, as indicated by the total absorption imagery. The derived patterns agree with those from concurrent surface drifters. For waters where CDOM overwhelmingly dominates the optical signal, however, the procedure tends to regard CDOM as the sole source of absorption, implying the need for better atmospheric correction and for adjustment of some model coefficients for this particular region.

Keywords: remote sensing, ocean optics, Case-II water, bio-optical inversion algorithm, optimization

1. INTRODUCTION: ESTIMATION OF BIO-OPTICAL PARAMETERS FROM SPACE

Accurate estimates of large-scale bio-optical parameters of the ocean are critical for various studies. The parameters include phytoplankton pigment (mainly chlorophyll-a), colored dissolved organic matter (CDOM, also called Gelbstoff or yellow substance), and particulate concentrations. In shallow waters bathymetry and benthic optical properties also play a role. To date, for optically complex waters in shallow, turbid coastal environment there is no operational algorithm to retrieve these variables from satellite data (IOCCG, 2000).

There are generally two steps to derive the bio-optical parameters from satellite ocean color sensors. One, an atmospheric correction algorithm is used to remove the atmospheric path radiance and to estimate the diffuse attenuation coefficient. This is to obtain the spectral water leaving radiance, $L_w(\lambda)$. Two, a bio-optical algorithm is applied to estimate the bio-optical parameters from $L_w(\lambda)$. It is also possible to perform these two tasks simultaneously (e.g., Chomko and Gordon, 2001), but the computational requirement prohibits the operational use of the procedure. The Chomko and Gordon (2001) procedure is not applicable to Case II waters (Morel and Prieur, 1977).

Atmospheric correction of the Sea-viewing Wide Field-of-view Sensor (SeaWiFS, McClain et al., 1998) is based on the algorithm proposed by Gordon and Wang (1994) for clear Case I waters. Several other atmospheric correction algorithms have been adapted for turbid waters to overcome the difficulty of non-zero L_w values in the near-infrared atmospheric correction bands (Siegel et al., 2000; Arnone et al., 1998), and other alternatives have been proposed as well (Ruddick et al., 2000; Hu et al., 2000). The Arnone et al. (1998) approach is currently operationally applied as the default option in the SeaWiFS data processing software (SeaDAS version 4.3, <http://seadas.gsfc.nasa.gov>). It assumes a certain relationship between L_w in the 670, 765, and 865-nm bands, and then derives the aerosol properties (type and optical thickness) iteratively. Further discussion of these atmospheric procedures is beyond the scope of this study, which focuses on the application of bio-optical inversion algorithms.

Once $L_w(\lambda)$ is derived from the satellite sensor after atmospheric correction, an inversion algorithm is used to derive the inherent optical properties (IOPs) from $L_w(\lambda)$, based on the relationship that

* hu@marine.usf.edu; phone 1 727 5533987; fax 1 727 5531103; <http://imars.usf.edu>

$$R_{rs}(\lambda) = f[a(\lambda), b_b(\lambda), \Theta] \approx g \cdot b_b(\lambda) / [b_b(\lambda) + a(\lambda)], \quad (1)$$

where R_{rs} is the remote sensing reflectance defined as L_w/E_d . E_d is the downwelling irradiance just above the sea surface. In the equation f is a function while g a constant. a and b_b are the total absorption and backscattering coefficients, respectively. They are the sum of the various water constituents: $a = a_w + a_p + a_g$ and $b_b = b_{bw} + b_{bp}$, where w stands for water molecules, a_p is for pigment, a_g is for Gelbstoff, and b_{bp} is the particle backscattering coefficient.

There are basically three types of bio-optical inversion algorithms to estimate the bio-optical parameters or IOPs (right-hand side of Eq. (1)) from the measured L_w or R_{rs} spectra. The first, and also the simplest, is a band-ratio algorithm (e.g., Gordon and Morel, 1983 for CZCS; O'Reilly et al., 1998 and O'Reilly et al., 2000 for SeaWiFS). Because phytoplankton pigment and CDOM absorb more light in the blue than in the green, the blue/green radiance ratio decreases with increasing concentrations. An empirical relationship can be established between the radiance ratio and the concentration from field data. For example, CZCS pigment concentration ($[C]$, mg/m³) was estimated as

$$\begin{aligned} [C] &= 1.13 \times (nLw_{443}/nLw_{550})^{-1.71} \text{ for } [C] < 1.5 \text{ mg/m}^3 \\ [C] &= 3.33 \times (nLw_{520}/nLw_{550})^{-2.44} \text{ for } [C] \geq 1.5 \text{ mg/m}^3, \end{aligned}$$

where "nLw" is the normalized water-leaving radiance, i.e., the nadir L_w with nadir solar illumination in the absence of the atmosphere. The OC2 algorithm (O'Reilly et al., 1998) estimated chlorophyll-*a* concentration ($[chl\ a]$, mg/m³) as

$$[chl\ a] = -0.0929 + 10^{0.2974 - 2.2429X + 0.8358X^2 - 0.0077X^3},$$

where $X = \log(R_{rs490}/R_{rs555})$ and F_0 is the solar constant. The OC4 algorithm (O'Reilly et al., 2000) estimated $[chl\ a]$ as

$$[chl\ a] = 10^{0.366 - 3.067X + 1.93X^2 + 0.649X^3 - 1.532X^4},$$

where $X = \log[\text{Max}(R_{rs443}, R_{rs490}, R_{rs510})/R_{rs555}]$. These empirical formulae are simple, but they don't distinguish between optical constituents, such as CDOM from chlorophyll. Therefore they are generally not applicable for turbid coastal waters, which are typically Case II (Morel and Prieur, 1977).

The second type of inversion algorithm is semi-analytical (e.g., Garver and Siegel, 1995; Carder et al., 1999) because analytical and empirical formulae are used to obtain the spectral absorption and backscattering coefficients of various water constituents. The Carder et al. (1999) algorithm uses three bands at 412, 443, and 555 nm to separate CDOM from chlorophyll based on the strong absorption at 412 nm by CDOM. Briefly, the algorithm assumes a hyperbolic tangent function to model the pigment absorption ($a_p(\lambda)$), an exponential function to model the Gelbstoff absorption ($a_g(\lambda)$), an empirical relationship to model the particle backscattering ($b_{bp}(\lambda)$), and an empirical relationship between R_{rs} (412, 443, 555) to derive $a_p(675)$, a_g and b_{bp} . $a_p(675)$ is then used to estimate $[chl\ a]$. The algorithm is currently operationally applied as a primary option to process data from the Moderate Resolution Imaging Spectroradiometer (MODIS, Salomonson et al. 1989). Applications of the algorithm to SeaWiFS data (Hu et al., in press; Hu et al., submitted) showed improved chlorophyll estimates for CDOM-rich waters. However, in extremely turbid or dark waters it often fails due to the extreme R_{rs} values found in these waters.

Another type of inversion algorithm can be generally referred to as "optimization" (e.g., Doerffer and Fischer, 1994; Lee et al., 1999). The parameters in the algorithm, such as $[chl\ a]$ (or a_p), a_g , suspended sediment concentration (or b_{bp}), bottom depth, bottom reflectance, etc., are tuned until the least root-mean-square error is reached between modeled (using equations similar to Eq. (1)) and measured spectra. The Lee et al. (1999) algorithm, designed for hyperspectral sensors, has been proven robust in applications to AVIRIS data to derive bathymetry and bottom albedo (Lee et al., 2001). It has also been applied to shallow-water SeaWiFS imagery (the Bahamas Banks) and showed preliminary success (Hu et al., 1998). The limitation of this type of approach is the requirement of enormous computational time, which presents an obstacle for efficient operational processing of satellite imagery. However, recent advances in optimization techniques showed significant improvement in computational speed so that a full-resolution SeaWiFS scene (~1285×4000 pixels) can be processed in ~1 hour.

Due to the complexity and seasonal variability in river plume and coastal waters, the band-ratio scheme often performs poorly (Hu et al., 2002). The semi-analytical algorithm improves ocean color estimates, but the performance is affected by the extreme signals found in these waters (e.g., very small L_w values in the blue). In this study, we

implemented the Lee et al. (1999) optimization algorithm and tested it over the turbid coastal waters in the Florida Bight where “black water” (SWFDOG, 2002) has been reported in spring 2002.

2. METHOD: IMPLEMENTATION OF THE OPTIMIZATION MODEL AND APPLICATION TO SEAWIFS DATA PROCESSING

The Lee et al. (1999) algorithm was originally implemented in Microsoft Excel to use its Solver routine to process discrete sampling stations. There was some difficulty to find an efficient non-linear optimization algorithm to process large volume of satellite data until late 2000 when a commercial computer library was purchased for such purpose. IDL and Visual basic programs have been developed to link the satellite data files (usually in HDF format) and the commercial library.

$nLw(\lambda)$ from the six visible bands of SeaWiFS, namely 412, 443, 490, 510, 555, and 670 nm, were used as the input of the optimization model. The principle of the inversion model has been described in detail in Lee et al. (1999). Similar to the study of Lee et al. (2001), several assumptions were made:

- 1) The Gelbstoff absorption spectral slope, S ($a_g(\lambda) = a_g(443) \exp [-S(\lambda-443)]$), was assumed to be 0.015 (Bricaud et al. 1981);
- 2) The particle backscattering spectral slope, Y , ($b_{bp}(\lambda) = b_{bp}(400) (400/\lambda)^Y$), was assumed to be 0.5 (Sathyendranath et al., 1989; Lee et al., 1999);
- 3) The spectral shape of the pigment absorption was modeled with a single-parameter function that allows the shape to change with the magnitude (Lee et al., 1999).

Other parameters, such as those affected by solar-viewing geometry, were assumed to be fixed using the same approach as in Lee et al. (2001).

The model has an option to add a shallow water bottom. Because the water in this study is turbid, this option was not chosen.

The model has been applied to process the SeaWiFS Level-3 (map-projected spectral water-leaving radiance) data products from late 2001 to spring 2002 over the Southwest Florida coastal waters. The results were used in part to study the “black water” event reported in early spring 2002 (SWFDOG, 2002).

3. RESULTS AND DISCUSSION

Figure 1 shows the SeaWiFS images taken on 9 January and 4 February 2002, respectively. Figs. 1a and 1b show the RGB composites using the Level-1 data (R: 670nm, G: 555nm, B: 412nm) while Figs. 1c and 1d show the RGB composites using Level-3 nLw data (R: 555nm, G: 490nm, B: 443nm). The dark, brownish water patches in the Florida Bight were reported as “black water.” Figure 2 shows the absorption and backscattering images obtained with the optimization model for the two dates. The RGB images indicate that the dark water patch is much larger on the 4 February image. However, when the color effects caused by turbidity (using backscattering as proxy) are removed (Figs. 2c and 2d), the total absorption images suggest that the water in the Florida Bight is similar for the two dates, except near the Everglades river mouths. The color contrasts between the two dates, as shown in Fig. 1, are mainly due to the changes in turbidity caused by some episodic events such as storm or strong wind. The absorption property is rather stable and consistent through time.

The performance of the model is evaluated with a RMS error parameter that describes the difference between the modeled and measured (i.e., SeaWiFS derived) nLw or R_{rs} spectra: $err = [\sum (R_{rs}^{modeled} - R_{rs}^{measured})^2]^{0.5} / \sum R_{rs}^{measured}$, where the summation is for all bands. The err images for the two dates are shown in Figure 3, while the spectra for several pixels of the 4 February image (Fig. 2d) are shown in Figure 4. For oligotrophic waters such as Pixel 1, the modeled spectrum matches the SeaWiFS data almost perfectly that the RMS error is < 2%. For more colored waters such as Pixels 2 and 3, the performance is still excellent although the RMS increases. However, when water is overwhelmingly dominated by CDOM, the model tends to approach the limit in the a_p estimates – 0.001 m^{-1} . The relatively large RMS errors for the extremely turbid water indicate the need for fine-tuning of the model coefficients for this complex region.

Water movement patterns in the Florida Bight can be derived from the absorption images in Figs. 2a and 2b. Fig. 2a suggests that the water from the Shark River and Everglades rivers first moved southwestward, and then turned to move westward at about 25°N 81.6°W until reaching west of 82°W . This agrees with data from concurrent surface drifter released near the river mouths on 11 November 2001 (Fig. 2a). Note that while the drifter track contains 2-month data, the satellite image is just a “snapshot” of the cumulated water movement effects. This explains the slight difference

between the colored stripe and the drifter track. Indeed, if we examine the 2-month time-series images after 11 November, better agreement is found between the ocean color patterns and the drifter locations before this date. Figure 5a shows the absorption image on 17 December 2001, when the ocean color pattern agrees closely with the drifter locations before this date. The colored patch west of the 8 December 2001 drifter location was pushed by the southeastward coastal current to result in the pattern seen on 9 January 2002. One day later, this pattern is seen moving southeastward, as shown on Fig. 5b. Fig. 2b also shows a pair of cyclonic and anti-cyclonic eddies, with the latter confirmed by numerical circulation models (Drs. Robert Weisberg and Ruoying He, USF, personal comm.).

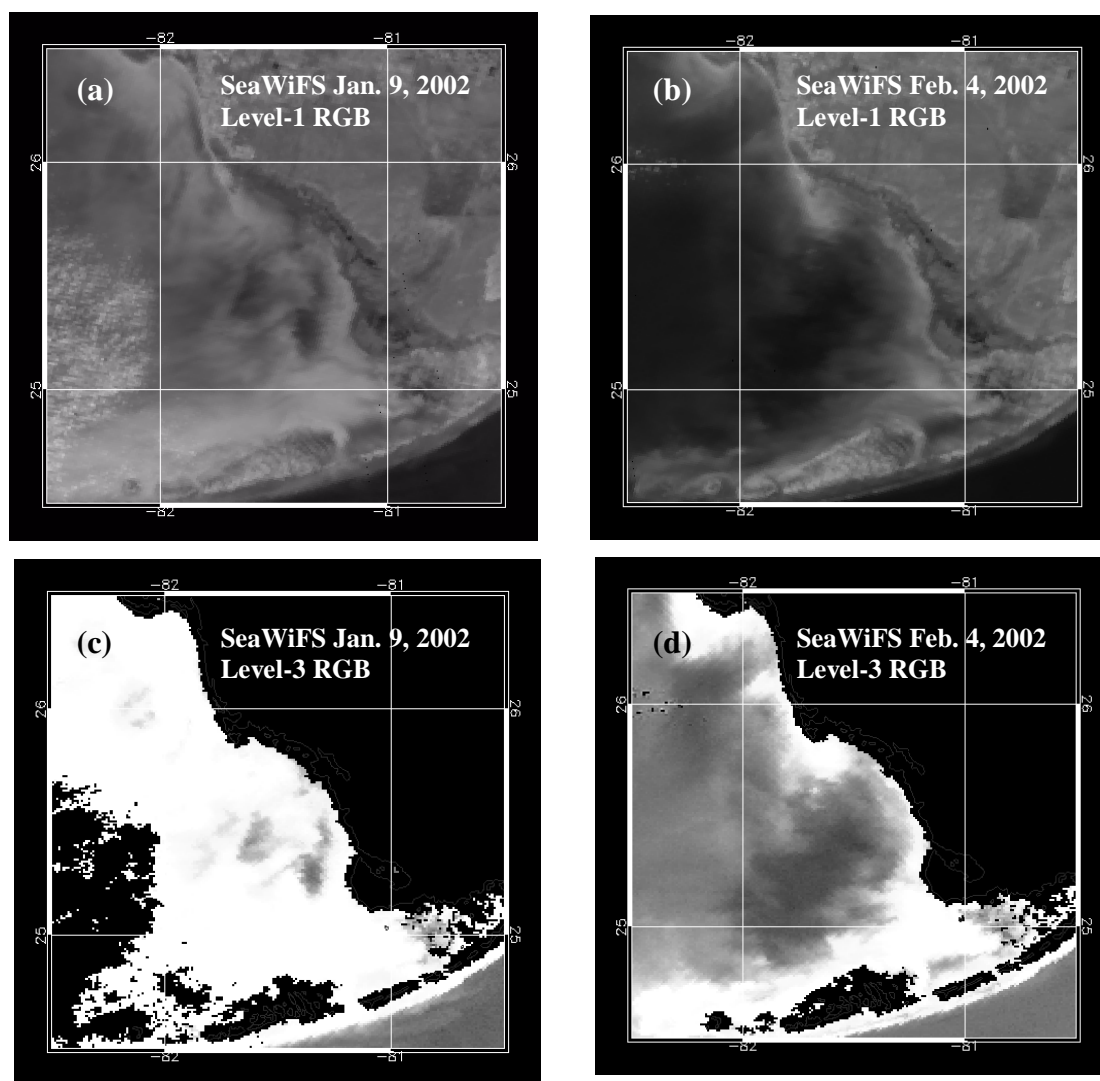


Figure 1. True color (RGB) SeaWiFS images on 9 January and 4 February 2002, respectively. (a) and (b): Level-1 composites (R: 670nm, G: 555nm, B: 412nm); (c) and (d): Level-3 composites (R: 555nm, G: 490nm, B: 443nm).

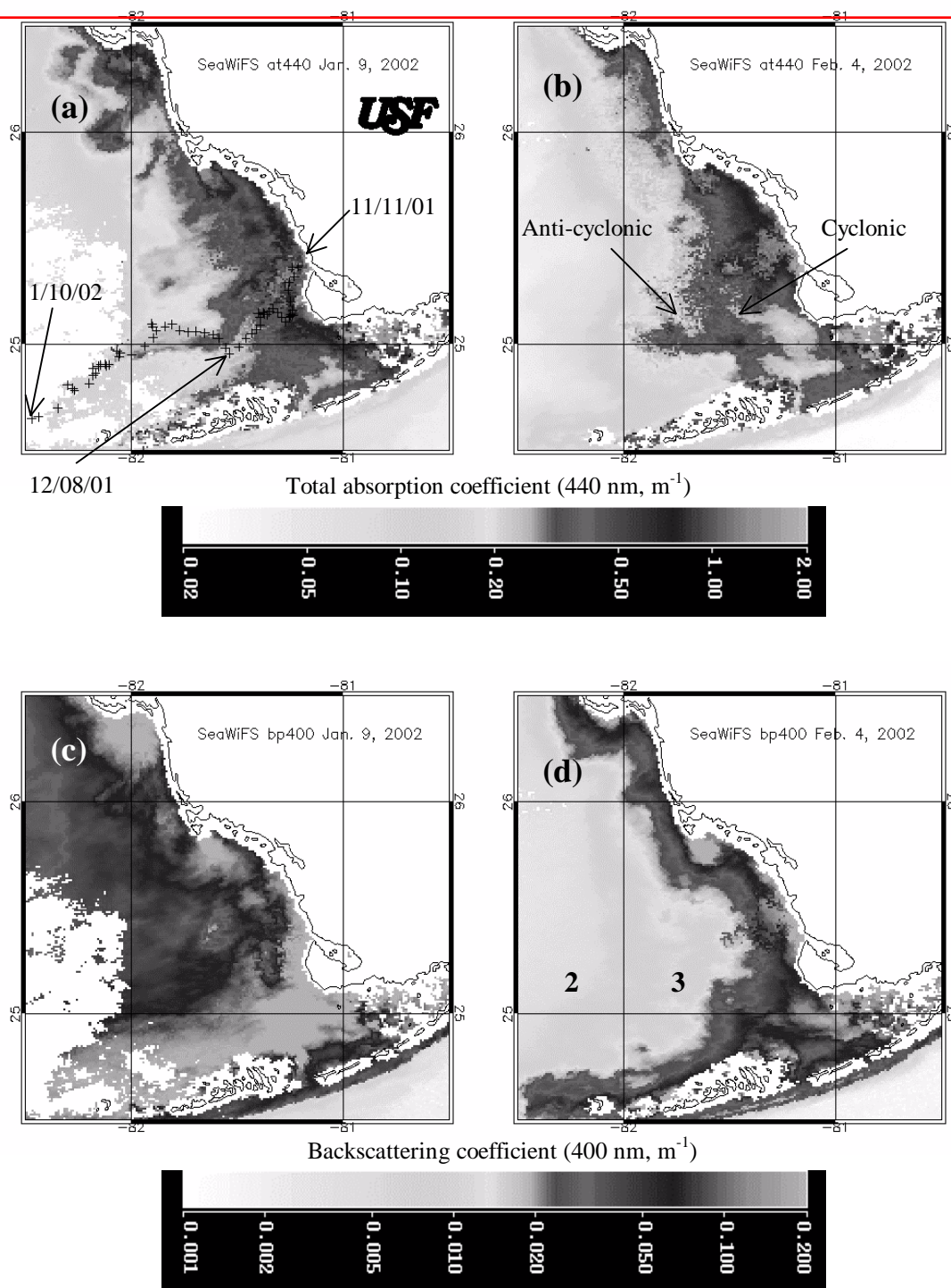


Figure 2. Total absorption coefficient (440 nm, m^{-1}) and particle backscattering coefficient (400nm, m^{-1}) derived with the optimization model. Overlaid on (a) are the daily surface drifter tracks from 11 November 2001 to 10 January 2002 (data courtesy of Drs. Elizabeth Johns and Tom Lee).

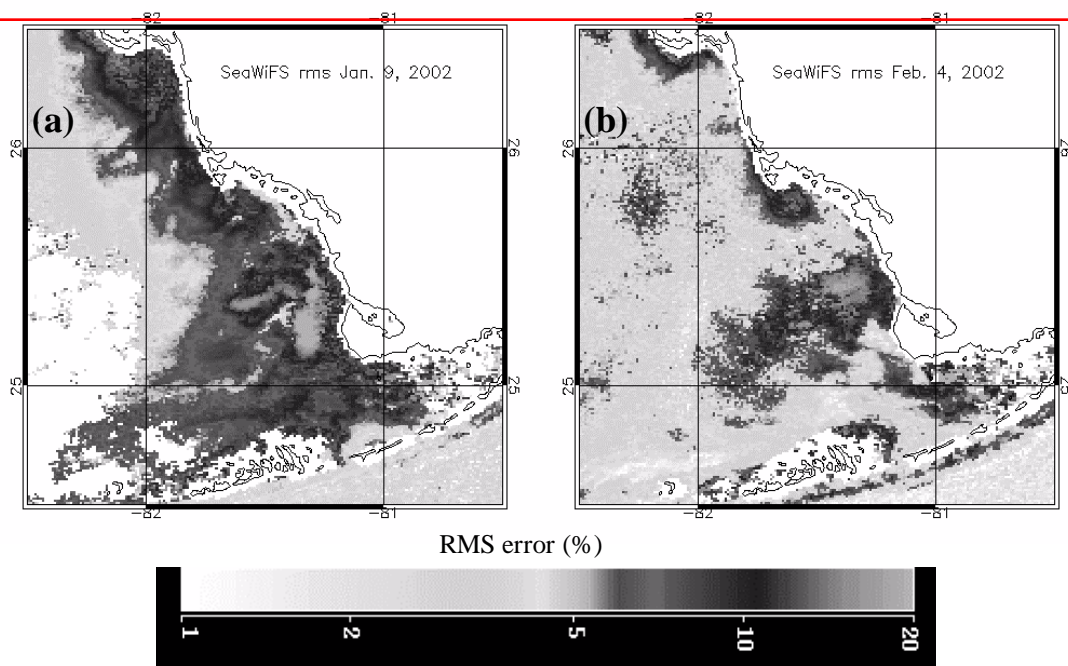


Figure 3. RMS error of the modeled spectra, as compared with the measured (i.e., SeaWiFS derived) spectra.

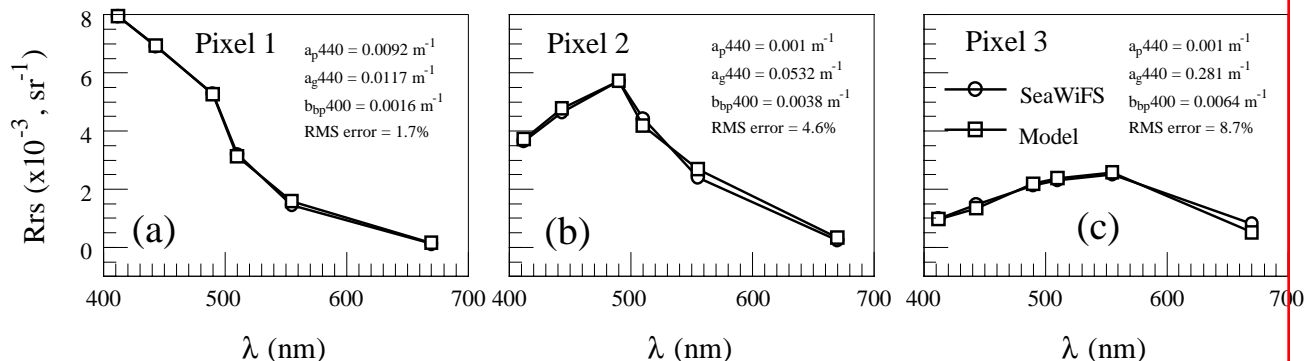


Figure 4. Comparison of the modeled and measured spectra for the three pixels from oligotrophic water, Gulf of Mexico water, and "black water", respectively (pixel locations shown in Fig. 2d).

Figure 6 shows the total absorption image on 28 March 2002, overlaid with locations of nearly concurrent sampling stations (samples were taken on 29 and 30 March). For the six stations, the comparison between the model-derived and the *in situ* measured a_{g440} is presented in Figure 7. The agreement for Stations 1 and 6 is excellent. For the dark water patches the retrieved a_{g440} also has acceptable accuracy (error < 35%. This is the uncertainty limit for [chl *a*] specified in NASA mission goals). Despite the slight difference for Stations 2-5, the trend is similar. The difference may be due in part to the lack of strict concurrency in the two data sets.

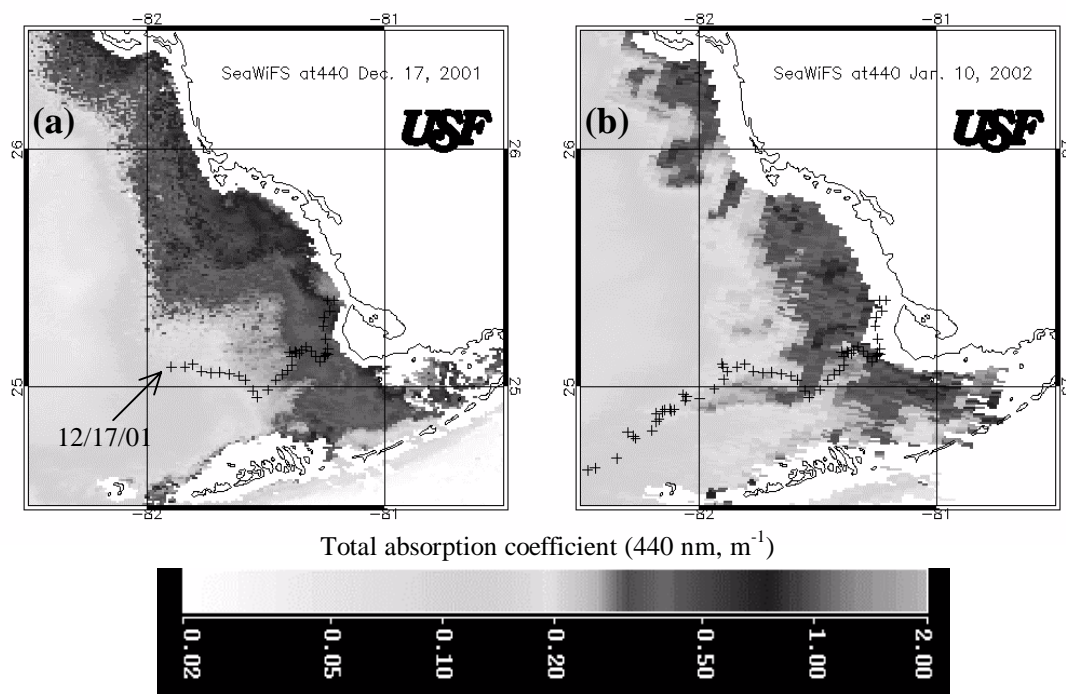


Figure 5. Total absorption coefficient (440 nm, m^{-1}) for 17 December 2001 and 10 January 2002, respectively. Overlaid on the images are the daily surface drifter tracks.

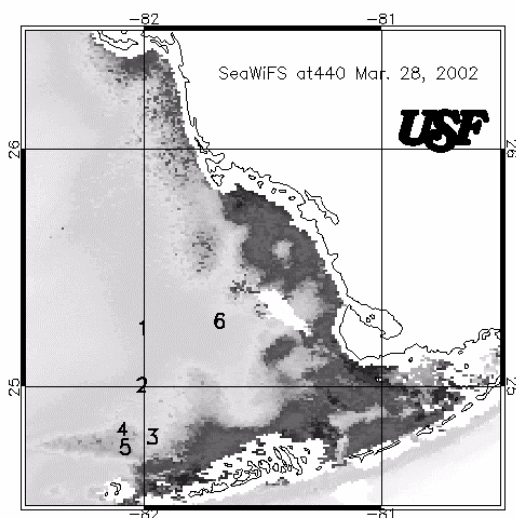


Figure 6. Total absorption coefficient (440 nm, m^{-1}) for 27 March 2002. Overlaid are the locations of nearly concurrent (29 and 30 March) sampling stations.

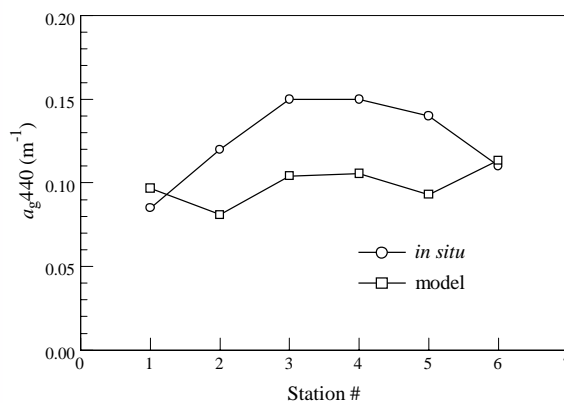


Figure 7. Comparison of CDOM absorption coefficient (a_{g440} , m^{-1}) derived from the model and from the *in situ* measurement in late March (station locations shown in Fig. 6).

The above results show that when CDOM absorption is several times larger than pigment absorption, the model is insensitive to small changes in pigment absorption, and therefore often fails to estimate this parameter. There are several possible reasons to cause this effect, among them including: erroneous sensor calibration and/or atmospheric correction. The SeaWiFS data used in this study were Version 4 data (SeaDAS4.3) that were processed with updated calibration and atmospheric correction (Arnone et al., 1998). The analysis with previous version shows that the model is very sensitive with these changes. Figure 8 shows the spectral comparison similar to those in Fig. 4, but the SeaWiFS data were Version 3. Not only is the RMS error bigger for all pixels, but also the derived bio-optical parameters are quite different. The current SeaWiFS data processing uses the Arnone et al. (1998) atmospheric correction method which assumes a fixed relationship between $R_{rs}(670, 765, 865\text{nm})$. This relationship may no longer hold with high [chl *a*] waters that strongly absorb light at 670 nm and fluoresce at 683nm. Further, the coefficients used in the model assumptions, especially the CDOM absorption and particle backscattering spectral slope parameters, may need to be adjusted according to *in situ* measurements. Nevertheless, it is clear that under most circumstances the total absorption and backscattering parameters can be successfully estimated with the optimization model, resulting in small (<5%) RMS errors in the modeled spectra. The estimated CDOM values also agreed well with those obtained *in situ*. The ability to partition backscattering from total absorption makes it possible to trace water movement patterns in coastal waters, as indicated by the consistent time-series images in the Florida Bight. In contrast, the variability in satellite ocean color signal is mainly caused by changes in turbidity, induced by episodic events. The retrieved backscattering parameter can be used to study sediment transport and resuspension, therefore is of great importance to biogeochemical studies.

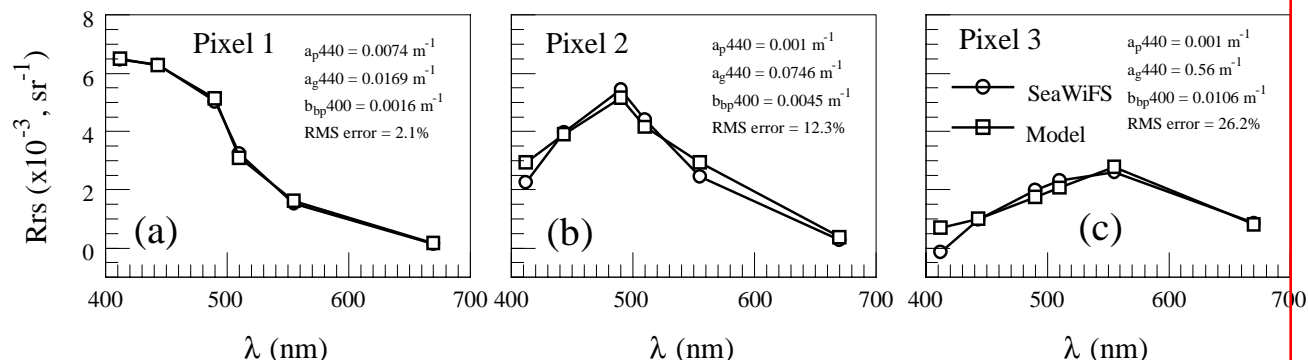


Figure 8. Similar to Fig. 4, but SeaWiFS Version 3 data were used.

4. CONCLUSION

A spectra-matching optimization model has been implemented to process SeaWiFS ocean color data to estimate inherent optical properties (absorption and backscattering) for both Case I and Case II waters. It is computationally efficient to process a full-resolution SeaWiFS image ($\sim 1285 \times 4000$ pixels) in ~ 1 hour, therefore can be used operationally for SeaWiFS data processing.

The total absorption and backscattering coefficients for the Florida Bight have been successfully retrieved with the model, as indicated by 1) small RMS errors in the modeled spectra (generally <5%), as compared with the SeaWiFS spectra; 2) good agreement between modeled and *in situ* CDOM absorption (<35% difference for a_{g400} between 0.08 and 0.15 m^{-1} . The latter is 10 times larger than those from adjacent clear water); 3) good agreement between the water movement patterns derived from the model and from the concurrent surface drifter; 4) consistency in the derived total absorption property through time, even though episodic turbidity events occur.

For extremely turbid waters, the model often tends to regard CDOM as the sole source of absorption. This may be caused by several reasons, as discussed above. Further improvement is necessary to use more realistic atmospheric correction models as well as to use more realistic optimization model coefficients.

ACKNOWLEDGEMENTS

This work was supported by the US National Aeronautics and Space Administration (NASA Grant NAG5-10738). We thank Dr. Elizabeth Johns (NOAA/AOML) and Dr. Tom Lee (U. Miami/RSMAS) for providing the surface drifter data. We are also grateful to Ms. Jennifer Cannizzaro and Mr. Jim Ivey (USF) for sharing the *in situ* CDOM data.

REFERENCES

- Arnone, R. A., P. Martinolich, R. W. Gould Jr., R. Stumpf, and S. Ladner, "Coastal optical properties using SeaWiFS," *Proceedings, Ocean Optics XIV*, S. Ackleson and J. Campbell (eds.), Office of Naval Research, Washington, DC, 1998.
- Bricaud, A., A. Morel, and L. Prieur, "Absorption by dissolved organic matter of the sea in the UV and visible domains," *Limnol. Oceanogr.* **26**, pp. 43-53, 1981.
- Carder, K. L., F. R. Chen, Z. P. Lee, S. K. Hawes, and D. Kamykowski, "Semianalytic moderate-resolution imaging spectrometer algorithms for chlorophyll *a* and absorption with Bio-optical domains based on nitrate depletion temperatures," *J. Geophys. Res.* **104**, pp. 5403-5421, 1999.
- Chomko, R. M., and H. R. Gordon, "Atmospheric correction of ocean color imagery: Test of the spectral optimization algorithm with the Sea-viewing Wide Field-of-View Sensor," *Appl. Opt.* **40**, pp. 2973-2984, 2001.
- Doerffer, R., and J. Fischer, J., "Concentrations of chlorophyll, suspended matter, and gelbstoff in case II waters derived from satellite coastal zone color scanner data with inverse modeling methods," *J. Geophys. Res.* **99**, pp. 7457-7466, 1994.
- Garver, S. A., and D. A. Siegel, "Inherent optical property inversion of ocean color spectra and its biogeochemical interpretation. I. Time series from the Sargasso Sea," *J. Geophys. Res.* **102**, pp. 18607-18625, 1997.
- Gordon, H. R., and A. Y. Morel, "Remote assessment of ocean color for interpretation of satellite visible imagery: a review," Springer-Verlag, New York, pp. 114, 1983.
- Gordon, H. R., and M. Wang, "Retrieval of water-leaving radiance and aerosol optical thickness over the oceans with SeaWiFS: a preliminary algorithm," *Appl. Opt.* **33**, pp. 443-452, 1994.
- Hu, C., K. L. Carder, and F. E. Muller-Karger, "A method to derive optical properties over shallow waters using SeaWiFS," *Proceedings, Ocean Optics XIV*, S. Ackleson and J. Campbell (eds.), Office of Naval Research, Washington, DC, 1998.
- Hu, C., K. L. Carder, and F. E. Muller-Karger, "Atmospheric correction of SeaWiFS imagery over turbid coastal waters: a practical method," *Remote Sens. Environ.* **74**, pp. 195-206, 2000, and **75**, pp. 447, 2001.
- Hu, C., A. L. Odriozola, J. P. Akl, F. E. Muller-Karger, R. Varela, Y. Astor, P. Swarzenski, and J-M Froidefond, "Remote sensing algorithms for river plumes: A comparison," ASLO2002, Victoria, British Columbia, Canada, 10-14 June 2002.
- Hu, C., F. E. Muller-Karger, D. C. Biggs, K. L. Carder, B. Nababan, D. Nadeau, and J. Vanderbloemen, "Comparison of ship and satellite bio-optical measurements on the continental margin of the NE Gulf of Mexico," *Inter. J. Remote Sens.* In press.
- Hu, C., E. T. Montgomery, R. W. Schmitt, and F. E. Muller-Karger, "The Amazon and Orinoco River plumes in the tropical Atlantic and Caribbean Sea: Observation from space and S-PALACE floats," *Deep-Sea Res. II*, submitted.
- IOCCG, *Remote sensing of ocean colour in coastal, and other optically-complex, waters*. p. 140, Sathyendranath, S. (ed.), Reports of the international ocean-colour coordinating group, No. 3, IOCCG, Dartmouth, Canada, 2000.
- Lee, Z., K. L. Carder, C. D. Mobley, R. G. Steward, and J. S. Patch, "Hyperspectral remote sensing for shallow waters: 2. Deriving bottom depths and water properties by optimization," *Appl. Opt.* **38**, pp. 3831-3843, 1999.
- Lee, Z., K. L. Carder, R. F. Chen, and T. G. Peacock, "Properties of the water column and bottom derived from Airborne Visible Infrared Imaging Spectrometer (AVIRIS) data," *J. Geophys. Res.* **106**, pp. 11639-11651, 2001.
- McClain C. R., M. L. Cleave, G. C. Feldman, W. W. Gregg, S. B. Hooker, and N. Kuring, "Science quality SeaWiFS data for global biosphere research," *Sea Tech.* **39**, pp. 10-16, 1998.
- O'Reilly, J. E., S. Maritorena, B. G. Mitchell, D. A. Siegel, K. L. Carder, S. A. Garver, M. Kahru, and C. R. McClain, "Ocean color chlorophyll algorithms for SeaWiFS," *J. Geophys. Res.* **103**, pp. 24937-24953, 1998.
- O'Reilly, J. E. et al., "Ocean color chlorophyll *a* algorithms for SeaWiFS, OC2, and OC4: version 4," In: SeaWiFS Postlaunch Tech. Report Series (S. B. Hooker & E. R. Firestone Eds.), NASA Technical Memorandum 2000-206892, Vol. 11. Greenbelt, Maryland: NASA Goddard Space Flight Center (51pp), 2000.

- Ruddick, K. G., F. Ovidio, and M. Rijkeboer, "Atmospheric correction of SeaWiFS imagery for turbid coastal and inland waters," *Appl. Opt.* **39**, pp 897-912, 2000.
- Salomonson, V. V., W. L. Barnes, P. W. Maymon, H. E. Montgomery, and H. Ostrow, "MODIS: advanced facility instrument for studies of the Earth as a system," *IEEE Geosci. Remote Sens.* **27**, pp. 145-152, 1989.
- Sathyendranath, S., L. Prieur, and A. Morel, "A three-component model of ocean colour and its application to remote sensing of phytoplankton pigments in coastal waters," *Int. J. Remote Sens.*, **10**, pp. 1373-1394, 1989.
- Siegel, D. A., M. Wang, S. Maritorena, and W. Robinson, "Atmospheric correction of satellite ocean color imagery: The black pixel assumption," *Appl. Opt.* **39**, pp. 3582-3591, 2000.
- SWFDOG, "Satellite images track 'black water' event off Florida coast," *EOS, Transaction, AGU*, **83**, pp. 281, 285, 2002.